





# TOPCon, TOPCoRE or TOPCon<sup>2</sup>

## A Simulation-Based Efficiency Analysis

Nico Wöhrle<sup>1,\*</sup> , Johannes M. Greulich<sup>1</sup> , Armin Richter<sup>1</sup> , Andreas Wolf<sup>1</sup>,  
Jochen Rentsch<sup>1</sup>, and Stefan Rein<sup>1</sup> 

<sup>1</sup>Fraunhofer-Institute for Solar Energy Systems ISE, Freiburg, Germany

\*Correspondence: Nico Wöhrle, [nico.woehrle@ise.fraunhofer.de](mailto:nico.woehrle@ise.fraunhofer.de)

**Abstract.** As tunnel oxide passivated contact (TOPCon) cell technology has established itself as the dominant cell technology in global photovoltaic production, this study investigates competing architectures, including TOPCoRE (TOPCon with Rear Emitter), and local TOPCon<sup>2</sup> (passivated contacts on both sample sides), to identify paths for enhancing power output by improving the cells' front side. The authors conduct a comprehensive simulation analysis using Quokka3, with input parameters derived from internal measurements and published data. While pointing out the necessary surface parameters to achieve a certain cell efficiency evolution, the sensitivity of the cell concepts to wafer quality, base resistance, and minority carrier lifetime is evaluated. The results indicate that the TOPCoRE concept on p-type wafers can be a strong contender to the standard iTOPCon, reaching 26%+ efficiency, if equally high electrical wafer quality can be achieved. The findings highlight the importance of further optimization paths, with local Front Surface Fields or local front TOPCon layers, demonstrating potential efficiencies of up to 26.5% and more.

**Keywords:** TOPCon, Photovoltaic, Efficiency, Simulation, Wafer Quality

## 1. Introduction

As TOPCon [1] cell technology has established itself as the dominant cell technology in global photovoltaic manufacturing, manufacturers who start or upgrade their production are presented with multiple avenues for advancement. Consensus indicates that improving the TOPCon cell's front side represents the most promising target for enhancing power output. Consequently, competing architectures such as TOPCoRE [2] and local TOPCon<sup>2</sup> (with the index referring to tunnel-oxide passivation on both contacts of the cell) have emerged within the research and development community. We compare these cell designs purely from a simulation standpoint, showing parameter requirements for achieving efficiency improvements and their sensitivity to wafer quality. A full area TOPCon<sup>2</sup> concept was not pursued after initial investigation due to high optical absorption.

## 2. Experimental

The experimental part has been conducted entirely with Quokka3 [3] simulations. Input parameters are taken from internal measurements, ITRPV predictions [3], as well as published manufacturer numbers [4, 5]. For direct comparison input parameters are identical where the cell structure allows for it. The contact pitch, i.e. the metallization finger distance was always optimized. Based on recent experiments [6], the base resistance and Shockley-Read-Hall (SRH)

lifetime in standard high-quality Cz-Si material have shown little correlation, thus we varied them independently, in contrast to previous studies on Si:B [7]. The simulated cell designs are depicted in Figure 1. The TOPCoRE architecture on n-type substrate is considered to have a higher recombination at the p-type polycrystalline contact compared to the n-type poly-Si [8] and hence lower efficiency and is not considered here. The benefit of local rear TOPCon layers [9, 10] on the short-circuit current and bifaciality can be an additional benefit for all cell architectures investigated here.

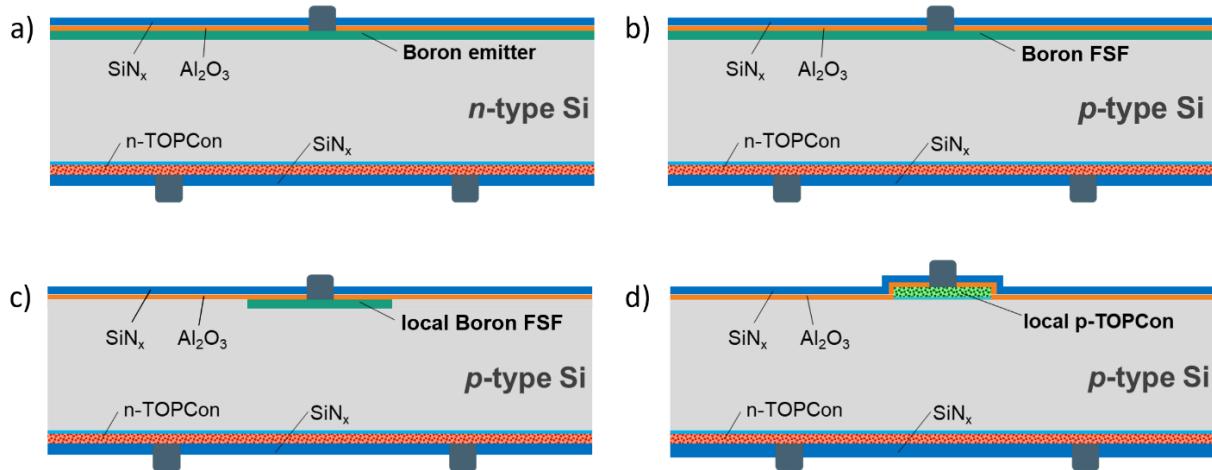


**Figure 1.** Schematic cross sections of (a) the iTOPCon cell concept, (b) the TOPCoRE cell concept, (c) the TOPCoRE concept with local FSF, and (d) the local TOPCon<sup>2</sup> cell concept

## 3. Results

### 3.1 Baseline

The first table shows a general comparison of the cell concepts under the base parameter set "25%-iTOPCon", meaning they share the parameter set wherever the architecture is shared. This is followed a sensitivity analysis to the wafer lifetime and base resistivity. Subsequently, we review the enhancement paths of each concept related to improved surfaces.

**Table 1.** Design comparison with "25%"-parameters on 1.5  $\Omega\text{cm}/10\text{ ms}$  SRH lifetime wafers.

Design	Wafer polarity	$j_{sc}$ (mA/cm <sup>2</sup> )	$V_{oc}$ (mV)	FF (%)	$\eta$ (%)
iTOPCon	n	41.6	723	82.9	25.0
TOPCoRE	p	41.4	723	83.7	25.1
TOPCoRE LFSF	p	Introduced later			
Local TOP-Con <sup>2</sup>	p	Introduced later			

The Free Energy Loss Analysis [11] for the iTOPCon cell, here in relative representation, shows that the front surface is the major loss channel at this stage with 68% of the electrical power loss. This is the reason why the front surface is our main focus in this work

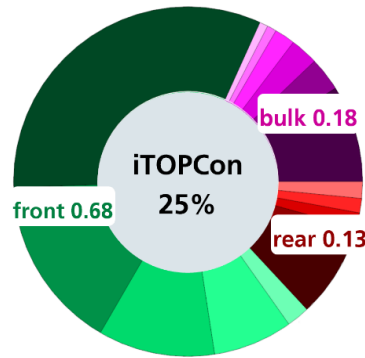


**Figure 2.** Relative electrical free energy losses for the 25% iTOPCon cell. The darkest green color represents the non-contacted front surface recombination. The other sub-groupings of similar color are not specified in detail

### 3.2 Reducing front recombination

In the steps 2-4, the improvement options of each concept are evaluated, mirrored in the simulations' surface parameters (Table 2). The full parameter set is given in the Annex.

**Table 2.** Input parameters for the considered cell concepts for the four development steps. The upgrade solution of a local FSF and local TOPCon<sup>2</sup> is already listed as well

Parameters	Dev. step 1	Dev. step 2	Dev. step 3	Dev. step 4
Finger width (screen printed)	27 $\mu\text{m}$	20 $\mu\text{m}$	17 $\mu\text{m}$	15 $\mu\text{m}$
Front contact resistance	2 $\text{m}\Omega\text{cm}^2$	1 $\text{m}\Omega\text{cm}^2$	0.9 $\text{m}\Omega\text{cm}^2$	0.8 $\text{m}\Omega\text{cm}^2$
Front contact recomb.	260 $\text{fA/cm}^2$	100 $\text{fA/cm}^2$	90 $\text{fA/cm}^2$	80 $\text{fA/cm}^2$
Front non-contact recombination	12 $\text{fA/cm}^2$	8 $\text{fA/cm}^2$	5 $\text{fA/cm}^2$	3.5 $\text{fA/cm}^2$
Front Rsheet	230 $\Omega/\text{sq}$	300 $\Omega/\text{sq}$	350 $\Omega/\text{sq}$	400 $\Omega/\text{sq}$
Rear TOPCon layer, contact recombination	5 $\text{fA/cm}^2$	5 $\text{fA/cm}^2$	5 $\text{fA/cm}^2$	4 $\text{fA/cm}^2$
<b>TOPCoRE local FSF</b>				
Front non-contact recombination (AlOx)	5 $\text{fA/cm}^2$	4 $\text{fA/cm}^2$	3 $\text{fA/cm}^2$	2 $\text{fA/cm}^2$
<b>Local TOPCon<sup>2</sup></b>				
Front TOPCon layer width	-	-	30-80 $\mu\text{m}$	30-80 $\mu\text{m}$
Front TOPCon non-contact & contact recombination	-	-	6-10 $\text{fA/cm}^2$	6-10 $\text{fA/cm}^2$
Rear TOPCon layer, non-contact recombination	-	-	0.8-2 $\text{fA/cm}^2$	0.8-2 $\text{fA/cm}^2$
Rear TOPCon layer, contact recombination	-	-	4-5 $\text{fA/cm}^2$	4-5 $\text{fA/cm}^2$

With the given parameter alterations, iTOPCon and TOPCoRE show a path from 25% well up to 26.3% for the 10 ms SRH lifetime wafer at 1.5  $\Omega\text{cm}$  base resistance (see Figure 3). TOPCoRE's small efficiency advantage (red line) is related to the p-type wafer with higher doping density leading to increased quasi-fermi-level split, reflected in higher  $V_{\text{oc}}$  (or increased  $FF$  if the pitch is adapted accordingly).

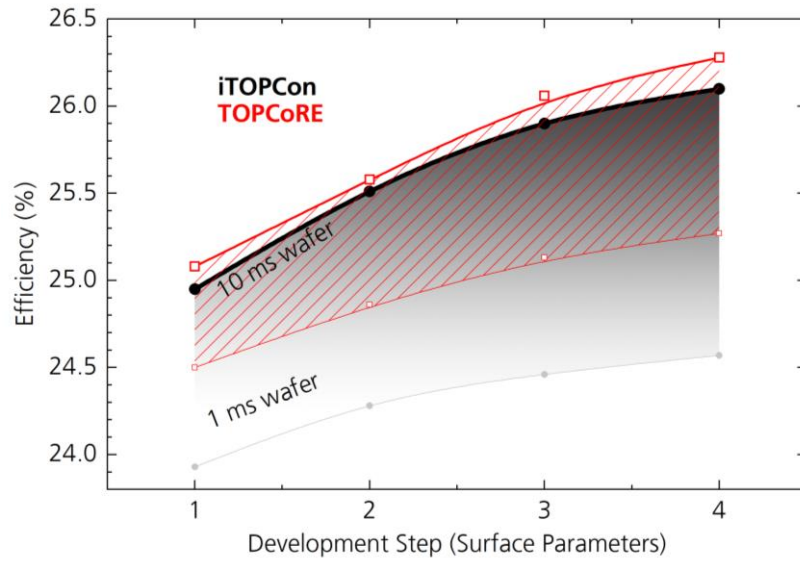


**Figure 3.** Development path with the altered cell parameters from Table 2 in four steps

For the same reason TOPCoRE is less affected by lower lifetimes as visible at the lower end of the corridors in Figure 3 comparing the same resistivity of p- and n-type wafers.

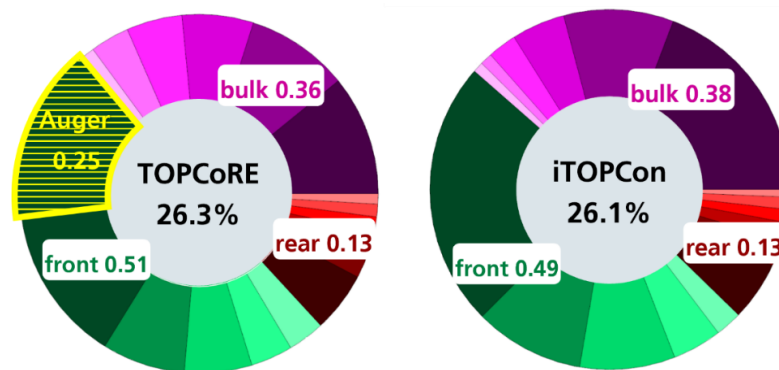


**Figure 4.** Relative electrical free energy losses for the TOPCoRE and TOPCon cell in development step 4 with 10 ms SRH lifetime

The Free Energy Loss Analysis shows, that although the front impact on the total losses has been reduced to ~50% of total electrical losses, it is still the major loss component for both concepts. Also, it shows that within the front recombination, Auger recombination (from the doped full area front surface field) is the main contributor to recombination. Consequently, it makes sense to reduce this area to the minimum, which is around the contact area. We cover two options shown in Figure 5 here.

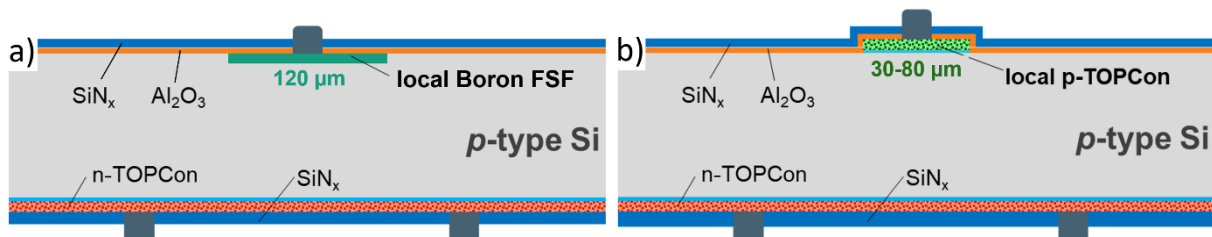


**Figure 5.** (a) TOPCoRE LFSF (local Front Surface Field). (b) TOPCoRE with second TOPCon layer beneath the front contact, "local TOPCon²"

One is a local Front Surface Field (LFSF), the second is a local TOPCon layer beneath the front contacts, resulting in a "Local TOPCon<sup>2</sup>" concept. Both concepts are an upgrade to the TOPCoRE cell on p-type wafer and both are in an early development stage. As before, the input values can be found in Table 2.

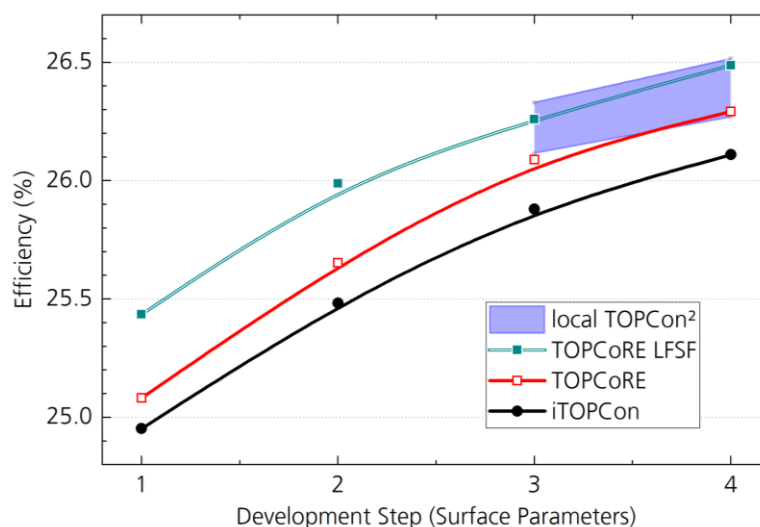


**Figure 6.** All four cell concepts compared over the four development steps. Local TOPCon<sup>2</sup> has a corridor instead of fixed values due to high uncertainty of assumed input parameters

A LFSF leads to an efficiency increase of  $\Delta\eta = 0.2\text{-}0.3\%$  over TOPCoRE with the full area FSF with otherwise equal cell parameters, driven by increased  $V_{oc}$ . Replacing the LFSF by a local TOPCon layer beneath the front contacts (blue area in Figure 6) also leads to increased efficiency over TOPCoRE (red line), but not necessarily more than the LFSF case. The reason for this is, that we did not see parameters for p-TOPCon layers so far, that improve significantly against a very good diffusion profile at the contacts. Also, the front TOPCon layer induces slightly worse optics where it is applied.

Arriving at 26% efficiency it is visible in the loss charts, that the bulk takes over the largest loss channel. Thus, wafer quality starts to become the bottleneck for cell efficiency again.

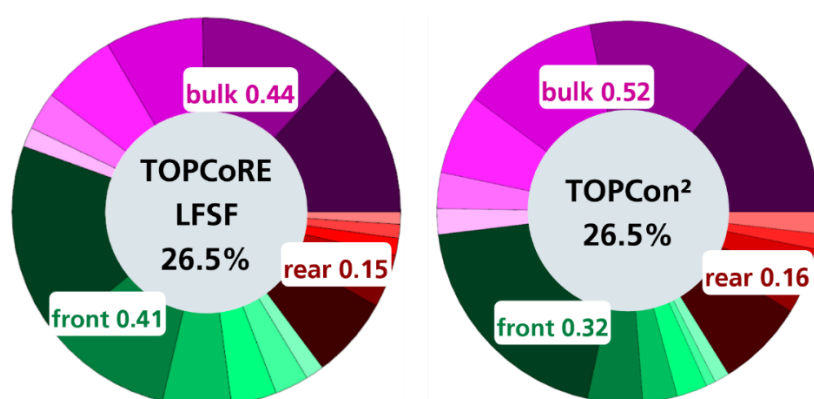


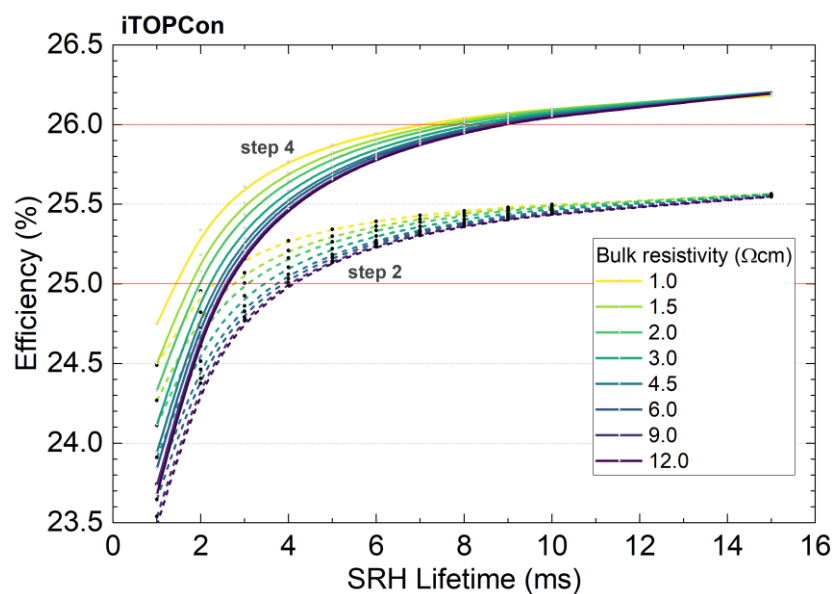
**Figure 7.** Relative electric free energy losses for the TOPCoRE LFSF and local TOPCon<sup>2</sup> cell in development step 4 with 10 ms SRH lifetime

## 4. Wafer Impact

For all simulations so far, it was assumed that the SRH lifetime of the wafers is 10 ms and the base resistivity is 1.5  $\Omega\text{cm}$  (for n- and p-type). To evaluate the wafer quality impact and the

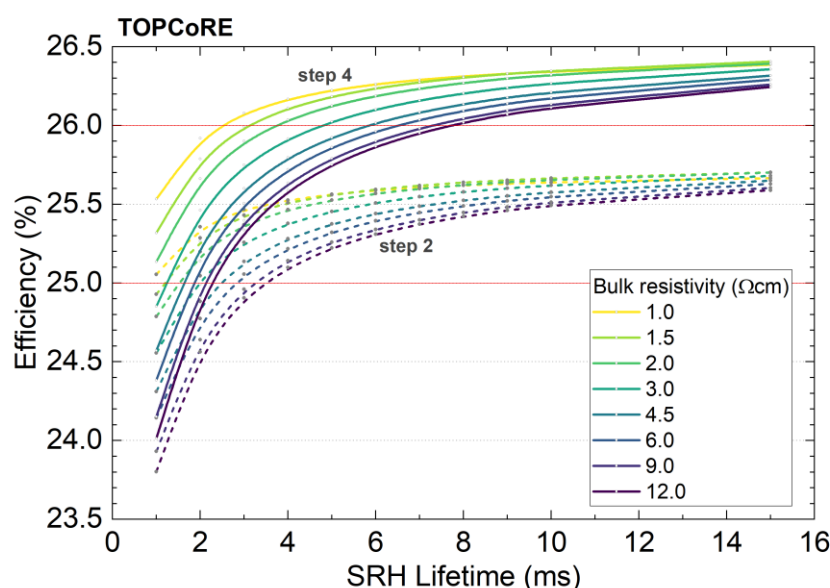
effect of resistivity variation on the cell efficiency, both were varied. Wafer specifications in manufacturing often state minimal SRH lifetimes of 1 ms, so we varied from 1 to 15 ms. Resistivity was varied from 1 to 12  $\Omega\text{cm}$ .

Figure 8 and Figure 9 plot these variations for the development step 2 and development step 4 of iTOPCon and TOPCoRE. The steep declines in efficiency, starting for SRH lifetimes of 5 ms and below, especially for cell setups with efficiency potential >25.5%, are evident. The n-type curve group (iTOPCon) seems to be more compact, i.e. more tolerant against base resistivity changes. However, it has steeper drops towards low SRH lifetimes, i.e. wafer quality. The p-type wafer (TOPCoRE) has wider efficiency spread over varied base resistivities, but is more tolerant against low lifetimes. This is due to comparing base resistivities. Equal base resistivities mean roughly a factor three in doping density between p- and n-type wafers. When comparing equal base doping densities – i.e. 1  $\Omega\text{cm}$  n-type with 3  $\Omega\text{cm}$  p-type, the efficiency differences between the two plots vanish almost entirely.



**Figure 8.** iTOPCon dependence on wafer quality for development step 2 and 4.





**Figure 9.** TOPCoRE offers higher lifetime tolerance for direct resistivity comparison with TOPCon (Figure 8), but it is more sensitive to higher resistivity materials

## 5. Discussion

iTOPCon on n-type and TOPCoRE on p-type wafers as fraternal twins have a head-to-head race for highest efficiencies over 26%. It should not be forgotten that other factors, such as wafer availability or intellectual property constraints, may play a role in deciding for one or the other wafer type. The stability of the wafer quality throughout the production chain will also contribute, since p-type is more susceptible to impurities such as iron. On the other hand, TOPCoRE poses the option of adding a local FSF, erasing a major loss channel at the front side, which facilitates a further efficiency gain of 0.2%. Local front-TOPCon layers showed a similar performance in the final parameter sets compared to a local FSF, both reaching 26.5% with input values which seem feasible for mass production. Both processes (local FSF and local TOPCon) have no established processing route for mass production so far, so no preference can be stated here. To reach these efficiencies, not only the surface quality, but also the wafer quality is crucial. We think that we will need to see higher SRH lifetimes in the future production to not only have high maximum efficiencies, but also reduce the production spread.

## 6. Conclusion

This study has demonstrated that the iTOPCon configuration on n-type wafers and the TOPCoRE design on p-type wafers are the leading candidates for achieving the highest photovoltaic efficiencies for single-junction silicon solar cells. Specifically, the iTOPCon architecture simulation has shown a maximum efficiency of 26.1%, while the TOPCoRE design reached an efficiency of 26.3%. Our simulations, which focused on the front side optimization, indicate that TOPCoRE has more upgrade options due to the rear emitter structure, namely with a local FSF or a local front TOPCon layer. Both variants achieved a gain of further 0.2% over TOPCoRE, reaching 26.5% efficiency. The findings underscore the critical need for further research into process optimizations that enhance the quality and performance of these advanced cell technologies in particular for the local FSF and local TOPCon<sup>2</sup> architecture. Overall, the streamlined development paths of iTOPCon and TOPCoRE and potentially local FSF or TOPCon<sup>2</sup> present the most promising strategies for advancing photovoltaic technology and improving energy conversion rates in future applications.

## Data availability statement

The datasets generated during and/or analysed during the current study are available from the corresponding author on reasonable request.

## Author contributions

Nico Wöhrle: Conceptualization, Data curation, Formal analysis, Investigation, Writing – original draft

Johannes Greulich: Conceptualization, Funding acquisition, Investigation, Project administration, Writing – original draft, Writing – review & editing

Armin Richter: Conceptualization, Data curation, Formal analysis, Investigation, Writing – review & editing

Andreas Wolf: Funding acquisition, Investigation, Supervision, Writing – review & editing

Jochen Rentsch: Investigation, Supervision, Writing – review & editing

Stefan Rein: Funding acquisition, Supervision, Writing – review & editing

## Competing interests

The authors declare that they have no competing interests.

## Funding

This work is supported by the German Federal Ministry for Economic Affairs and Climate Action within the projects “StroKoTOP” (grant no. 03EE1178A) and WaMTec (grand no. 03EE1193).

## References

- [1] F. Feldmann et al., “Passivated rear contacts for high-efficiency n-type Si solar cells providing high interface passivation quality and excellent transport characteristics,” *Sol. Energy Mater. Sol. Cells*, vol. 120, pp. 270–274, 2014, doi: <https://doi.org/10.1016/j.solmat.2013.09.017>
- [2] A. Richter et al., “Tunnel oxide passivating electron contacts as full-area rear emitter of high-efficiency p-type silicon solar cells,” *Prog Photovolt Res Appl.*, vol. 26, no. 8, p. 233506, 2018, doi: <https://doi.org/10.1002/ppp.2960>
- [3] A. Fell, “A free and fast three-dimensional/two-dimensional solar cell simulator featuring conductive boundary and quasi-neutrality approximations,” *IEEE Trans. Electron Devices*, vol. 60, no. 2, pp. 733–738, 2013, doi: <https://doi.org/10.1109/TED.2012.2231415>
- [4] ITRPV, “International Technology Roadmap for Photovoltaic (ITRPV): 2023 Results,” VDMA, 2023.
- [5] A. Mette et al., “Q.ANTUM NEO with LECO Exceeding 25.5 % cell Efficiency,” *Sol. Energy Mater. Sol. Cells*, vol. 277, p. 113110, 2024, <https://doi.org/10.1016/j.solmat.2024.113110>
- [6] J. Horzel et al., “High lifetime Ga-doped Cz-Si for carrier-selective junction solar cells,” *Solar RRL*, vol. 7, no.8, p. 2200613, 2023, <https://doi.org/10.1002/solr.202200613>



- [7] D. C. Walter et al., "Realistic efficiency potential of next-generation industrial Czochralski-grown silicon solar cells after deactivation of the boron-oxygen-related defect center," *Prog Photovolt Res Appl.*, vol. 24, no. 7, pp. 920–928, 2016, <https://doi.org/10.1002/ppa.2731>
- [8] Di Yan et al., "Polysilicon passivated junctions: The next technology for silicon solar cells?," *Joule*, vol. 5, no. 4, pp. 811–828, 2021, <https://doi.org/10.1016/j.joule.2021.02.013>
- [9] T. Sugiura et al., "Advanced Industrial Tunnel Oxide Passivated Contact Solar Cell by the Rear-Side Local Carrier-Selective Contact," *Electron Devices, IEEE Transactions on*, vol. 69, no. 5, pp. 2481–2487, 2022, <https://doi.org/10.1109/TED.2022.3159272>
- [10] W. Wan et al., "Enhancing passivation and reducing absorption losses in TOPCon solar cells via Poly-Si finger structure," *Sol. Energy Mater. Sol. Cells*, vol. 286, p. 113600, 2025, <https://doi.org/10.1016/j.solmat.2025.113600>
- [11] R. Brendel et al., "Theory of analyzing free energy losses in solar cells," *Appl. Phys. Lett.*, vol. 93, no. 17, p. 173503, 2008, <https://doi.org/10.1063/1.3006053>
- [12] T. Niewelt et al., "Reassessment of the intrinsic bulk recombination in crystalline silicon," *Sol. Energy Mater. Sol. Cells*, vol. 235, p. 111467, 2022, <https://doi.org/10.1016/j.solmat.2021.111467>

## Annex

**Table 3.** Full Input parameters for the considered cell concepts for the four development steps.

<b>Parameters</b>	<b>Dev. step 1</b>	<b>Dev. step 2</b>	<b>Dev. step 3</b>	<b>Dev. step 4</b>
Cell thickness	120 $\mu\text{m}$	120 $\mu\text{m}$	120 $\mu\text{m}$	120 $\mu\text{m}$
Finger width (screen printed)	27 $\mu\text{m}$	20 $\mu\text{m}$	17 $\mu\text{m}$	15 $\mu\text{m}$
Front contact resistance	2 $\text{m}\Omega\text{cm}^2$	1 $\text{m}\Omega\text{cm}^2$	0.9 $\text{m}\Omega\text{cm}^2$	0.8 $\text{m}\Omega\text{cm}^2$
Front contact recomb.	260 $\text{fA/cm}^2$	100 $\text{fA/cm}^2$	90 $\text{fA/cm}^2$	80 $\text{fA/cm}^2$
Front non-contact recombination	12 $\text{fA/cm}^2$	8 $\text{fA/cm}^2$	5 $\text{fA/cm}^2$	3.5 $\text{fA/cm}^2$
Front Rsheet	230 $\Omega/\text{sq}$	300 $\Omega/\text{sq}$	350 $\Omega/\text{sq}$	400 $\Omega/\text{sq}$
Rear TOPCon layer, contact recombination	5 $\text{fA/cm}^2$	5 $\text{fA/cm}^2$	5 $\text{fA/cm}^2$	4 $\text{fA/cm}^2$
Rear TOPCon layer, non-contact recombination	1 $\text{fA/cm}^2$	1 $\text{fA/cm}^2$	1 $\text{fA/cm}^2$	0.8 $\text{fA/cm}^2$
Rear poly thickness	80 nm	80 nm	80 nm	80 nm
Rear finger width	27 $\mu\text{m}$	20 $\mu\text{m}$	20 $\mu\text{m}$	20 $\mu\text{m}$
Rear contact resistance	2.5 $\text{m}\Omega\text{cm}^2$	1.5 $\text{m}\Omega\text{cm}^2$	0.9 $\text{m}\Omega\text{cm}^2$	0.8 $\text{m}\Omega\text{cm}^2$
Vertical resistance rear TOP-Con layer	15 $\text{m}\Omega\text{cm}^2$	15 $\text{m}\Omega\text{cm}^2$	15 $\text{m}\Omega\text{cm}^2$	15 $\text{m}\Omega\text{cm}^2$
j02	0 $\text{nA/cm}^2$	0 $\text{nA/cm}^2$	0 $\text{nA/cm}^2$	0 $\text{nA/cm}^2$
<b>TOPCoRE local FSF</b>				
Front non-contact recombination (AlOx)	5 $\text{fA/cm}^2$	4 $\text{fA/cm}^2$	3 $\text{fA/cm}^2$	2 $\text{fA/cm}^2$
<b>Local TOPCon<sup>2</sup></b>				
Front TOPCon layer width	-	-	30-80 $\mu\text{m}$	30-80 $\mu\text{m}$
Front TOPCon non-contact & contact recombination	-	-	6-10 $\text{fA/cm}^2$	6-10 $\text{fA/cm}^2$
Vertical resistance front TOP-Con layer	-	-	1-1.5 $\text{m}\Omega\text{cm}^2$	1-1.5 $\text{m}\Omega\text{cm}^2$
Rear TOPCon layer, non-contact recombination	-	-	0.8-2 $\text{fA/cm}^2$	0.8-2 $\text{fA/cm}^2$
Rear TOPCon layer, contact recombination	-	-	4-5 $\text{fA/cm}^2$	4-5 $\text{fA/cm}^2$
Vertical resistance rear TOP-Con layer	-	-	5-15 $\text{m}\Omega\text{cm}^2$	5-15 $\text{m}\Omega\text{cm}^2$

For all simulation the Auger model of Niewelt et al. [12] was used.